Water in the Small Bodies of the Solar System

David Jewitt and Lysa Chizmadia
University of Hawaii

Robert Grimm
Southwest Research Institute

Dina Prialnik
Tel Aviv University

Water is important for its obvious role as the enabler of life but more generally as the most abundant volatile molecule in the Solar system, containing about half of the condensible mass in solids. In its solid phase, water strongly influences the opacity of the protoplanetary disk and may determine how fast, and even whether, gas giant planets form. Water ice is found or suspected in a wide range of small-body populations, including the asteroids, the giant planet Trojan librators, Centaurs, comets and Kuiper belt objects. In addition to ice, there is mineralogical evidence for the past presence of liquid water in certain meteorites and, by inference, in their parent main-belt asteroids. The survival and evolution of liquid and solid water in small bodies is discussed.

Water is the driving force of all nature.

-Leonardo da Vinci

1. INTRODUCTION

Leonardo's claim is only a slight exaggeration. After hydrogen and helium, oxygen is the third most cosmically abundant element (H/O $\sim$1200 by number). Helium is chemically inert leaving hydrogen atoms free to combine to make H_2, or with oxygen to form H_2O. Water is the second most abundant molecule (after H_2) in those astrophysical environments where the temperature is below the thermal dissociation limit ($\sim$2000 K). These environments include almost the entire protoplanetary disk of the Sun. Therefore, it should be no surprise that water played an important role over a wide range of heliocentric distances in the Solar system from the region of the terrestrial planets out to the Kuiper belt and beyond.

At low temperatures, water is thermodynamically stable as a solid; it condenses as frost or ice. Ice grains have a strong influence on the mean radiative opacity (*Pollack et al.*, 1994) and so can change the temperature structure in the protoplanetary disk. In turn, the disk viscosity is related to the temperature of the gas. Hence, the freeze-out and distribution of icy grains together have a surprisingly strong impact on the transport of energy, mass and angular momentum and so influence the overall structure and evolution of the protoplanetary disk (*Ciesla and Cuzzi*, 2006).

The "snow line" (actually, it is a surface) divides the outer, cold, ice-rich region of the protoplanetary disk from the inner, steamy hot zone. Outward gas motions across the snow line result in the condensation of water into ice grains, which can collide, stick and grow until they dynamically decouple from the flow and are left behind. In this way, the snow line defines the inner edge of a cold trap in which the density of solids may have been sufficiently enhanced as to help speed the growth of planetesimals and, ultimately, of the cores of the giant planets (*Stevenson and Lunine*, 1988). Aerodynamic drag causes 100-meter scale ice-rich planetesimals from the outer disk to spiral inwards on very short timescales (perhaps 1 AU per century). Some are swept up by bodies undergoing accelerated growth just outside the snow line. Others cross the snow line to quickly sublimate, enhancing the local water vapor abundance. Coupled with on-going dissociation from ultraviolet photons, these freeze-out and sublimation processes lead to isotopic fractionation anomalies in water (*Lyons and Young*, 2005) that have already been observed in the meteorite record (*Krot et al.*, 2005). In the protoplanetary disk, opacity due to grains inhibited radiative cooling and raised the mid-plane kinetic temperature. Growth and migration of solids in the disk would have caused the opacity to change, so moving the snow line. For a fraction of a million years, it may have pushed in to the orbit of Mars or even closer (*Sasselov and Lecar*, 2000; *Ciesla and Cuzzi*, 2006 c.f. Fig. 1), meaning that asteroids in the main belt, between Mars and Jupiter, could have incorporated water ice upon formation. Indeed, small samples of certain asteroids, available to us in the form of meteorites, contain hydrated minerals that probably formed when buried ice melted and chemically reacted with surrounding refractory materials (*Kerridge et al.*, 1979; *McSween*, 1979). Short-lived radionuclides were the most probable heat source in the early Solar System. Cosmochemical evidence for ^{26}Al (half-life 0.71 Myr) is

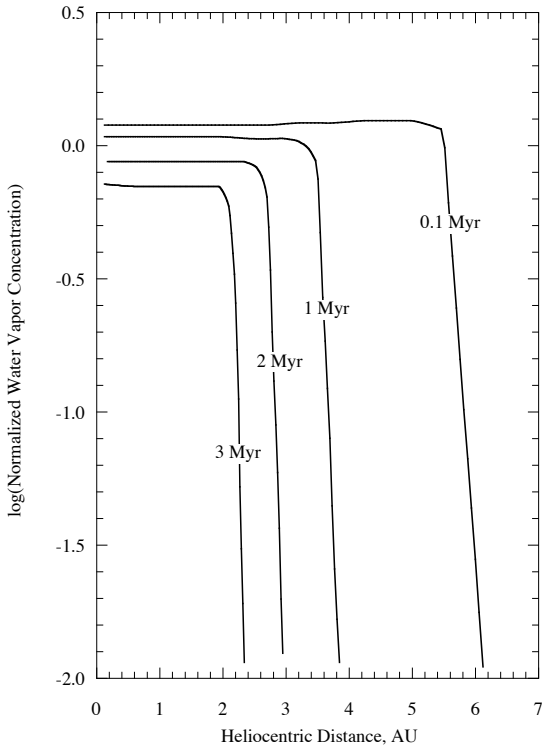

Fig. 1.— Results from a model of the temporal evolution of the water vapor content in the protoplanetary disk as a function of the heliocentric distance. The curves are labeled with the time since disk formation. The steep drop on each curve is caused by condensation of the vapor into ice grains, and marks the moving snow-line. These results are for one simplistic model of the protoplanetary disk and should not be taken literally. Their value is in showing the migration of the snow line in response to grain growth, gas drag and time-dependent opacity variations in the disk. Figure replotted from *Ciesla and Cuzzi* 2006.

firmly established (*Lee et al.*, 1976; see *MacPherson et al.*, 1995, for a review). Additionally, ^{60}Fe (half-life $\sim$1.5 Myr) may have provided supplemental heating (*Mostefaoui et al.*, 2004).

Further from the Sun the ice trapped in solid bodies may have never melted. This is mainly because the lower disk surface densities in the outer regions lead to long growth times. Small bodies in the outer regions, especially the Kuiper belt objects and their progeny (the Centaurs and the nuclei of Jupiter family comets), probably escaped melting because they did not form quickly enough to capture a full complement of the primary heating agent, ^{26}Al. Melting is nevertheless expected in the larger Kuiper belt objects, where the surface area to volume ratio is small and the longer-lived radioactive elements can play a role (see section 5).

As this preamble shows, the study of water in small Solar system bodies involves perspectives that are astronomical, geochemical and physical. As is common in science, the study of one broad subject is breaking into many smaller sub-fields that will eventually become mutually incomprehensible. Here, we aim to provide an overview that will discuss the most significant issues concerning water in the Solar system's small bodies in a language accessible to astronomers and planetary scientists, the main readers of this volume. We recommend the reader to earlier reviews of the astronomical aspects by *Rivkin et al.* (2002), of the thermal models by *McSween et al.* (2002) and of the meteorite record by *Keil* (2000).

2. EVIDENCE FROM THE METEORITES

2.1. Evidence for Extraterrestrial Liquid Water

Meteorites provide samples of rock from asteroids in the main-belt between Mars and Jupiter. Some contain evidence for the past presence of liquid water in the form of hydrated phases. Here, "hydrated" means that the mineral, or phase, contains structurally bound OH or H_2O, with chemical bonds between the OH/H_2O molecule and the other elements in the crystal. For example, in serpentine ($Mg_3Si_2O_5(OH)_4$) the OH molecule shares electrons with the SiO_4 tetrahedra and is an integral part of the mineral. Hydrated meteorites are those that contain hydrated phases and/or minerals which likely formed in the presence of an aqueous fluid. Not all minerals which formed as a consequence of liquid water contain OH or H_2O molecules. Hydrated meteorites include most groups of carbonaceous chondrites and some of the type 3 ordinary chondrites.

Evidence that the aqueous alteration of these meteorites occurred extra-terrestrially includes:

(i) Some of the meteorites were observed to fall and immediately recovered: not enough time elapsed for terrestrial alteration reactions to occur.

(ii) Radioisotopes in carbonate assemblages indicate formation $\sim$5 to 10 Myr after the solidification of the chondrules. Earth at this time was too hot to sustain liquid water.

(iii) The oxygen isotopic composition of different meteorite groups are distinct from each other and from Earth (*Clayton et al.*, 1976; *Clayton and Mayeda*, 1984; *Clayton*, 1993, 1999). Materials that form on Earth fall on the terrestrial fractionation line. The hydrated phases in chondrites do not fall on this line.

(iv) The Fe^{2+}/Fe^{3+} ratio in the secondary minerals is generally significantly higher than in secondary minerals that form on the surface of the Earth (*Zolensky et al.*, 1993). The surface of the Earth is much more oxidizing than the environment in which these reactions took place.

Several styles of aqueous alteration have been proposed (Fig. 2). Gas phase hydration reactions and the condensation of carbonate were initially thought, on theoretical grounds, to be kinetically inhibited (*Prinn and Fegley*, 1987). However, minerals including calcite and dolomite have been found in the dust ejected from old stars (e.g., *Kemper et al.*, 2002) where gas phase reactions are now thought possible (*Toppani et al.*, 2005). Similar reactions as well as hydration reactions may have occurred in the

cooling Solar nebula, perhaps aided by shock heating and compression (*Ciesla et al.*, 2003). Evidence consistent with gas-phase alteration comes from the fine-grained rims of chondrules. Alternatively, or in addition, alteration by liquid water could have occurred in the parent asteroids following the melting of buried ice by heat liberated by radioactive decay. Evidence for aqueous alteration involving liquid water comes from geochemical and textural evidence in the carbonaceous chondrites. For example, the systematic redistribution of elemental constituents on scales of millimeters (e.g., Mg and Ca into the matrix and Fe into the chondrules (*McSween*, 1979)) is best explained by liquid water. The consistent degree and state of alteration of chondrules with similar compositions in the same chondrites is also difficult to understand in the context of gas-phase processing but would be naturally produced by aqueous alteration (e.g., *Hanowski and Brearley*, 2001). Furthermore, mineral veins and Fe-rich aureoles indicate soaking in a fluid for an extended period of time (*Zolensky et al.*, 1989, 1998; *Browning et al.*, 1996; *Hanowski and Brearley*, 2001). A reasonable view is that gas-phase alteration probably occurred, but post-accretion alteration by liquid water played a larger role, often overwhelming any products of gas-phase alteration (*Brearley*, 2003). The distribution of hydrated materials within an asteroid is likely to be further complicated, during and after the hydration phase, by brecciation, impact shattering and re-arrangement (Fig. 2).

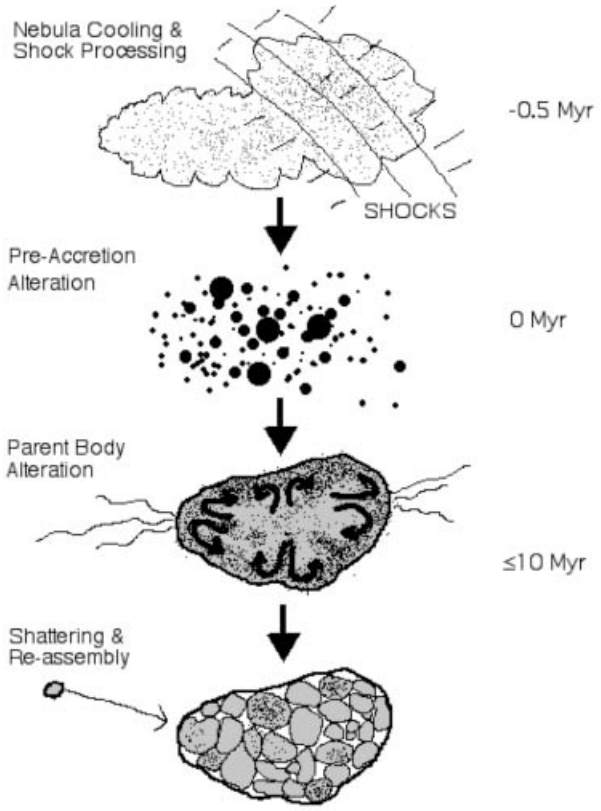

Fig. 2.— Cartoon showing possible stages in the evolution of water in a growing small body. A: Nebula cooling and shock processing occur as the protoplanetary nebula cools by radiation into space but is briefly shocked to higher temperatures and densities. B: Pre-accretion alteration occurs in small precursor bodies that later mix with others (perhaps from far away in the disk) to form the final parent body. C: Parent body alteration involves the flow of water through the formed asteroid or comet. D: Later, collisional shattering and re-assembly under gravity introduces macroporosity and chaotically jumbles the hydrated materials with others. Rough times are noted relative to the solidification of the CAIs.

2.2. Carbonaceous Chondrites

Several observations indicate contact with water. Most directly, the bulk rock contains H_2O when analyzed (e.g., carbonaceous chondrites can contain up to 12 wt% H_2O). Secondary minerals containing structurally bound OH/H_2O are also present, as are minerals which generally form in the presence of liquid H_2O. The oxygen in hydrated minerals is ^{16}O poor compared to the primary minerals, such as olivine, indicating that the water/ice must have formed at a different time or place from the primary phases (*Clayton and Mayeda*, 1999). O-isotopes are distinct between different bodies and groups of meteorites. Since we know that some of these bodies formed at different distances from the Sun (e.g., Earth, Mars, (4) Vesta), the O-isotopes imply that different regions of the Solar nebula had different O-isotopic compositions.

Water-related secondary minerals are mainly clays with related serpentine (Fig. 3), carbonates (Fig. 4), phosphates, sulphates, sulphides, and oxides. Carbonates, phosphates, sulphates, sulphides and oxides formed under oxidizing conditions unlike the H_2-rich, reducing Solar nebula, and generally precipitate from liquid water. Some of these are found in cross-cutting relationships with other phases, indicating that they must have formed later (Fig. 5). We briefly discuss important secondary minerals that imply the action of liquid water in meteorite parent bodies.

Clay minerals and serpentines contain structurally bound OH (Fig. 3). The aqueous alteration of CM chondrites is thought to have occurred at $\sim$20°C (*Clayton et al.*, 1976; *Clayton and Mayeda*, 1984; *Clayton*, 1993, 1999; *Zolensky et al.*, 1993).

Carbonates, such as calcite ($CaCO_3$) and dolomite ($CaMgC_2O_6$), are often present in the most aqueously altered carbonaceous chondrites, the CMs and the CIs. It is unlikely that the partial pressure of CO_2 gas was high enough in the nebula for carbonate to have formed. Origin in solution is more plausible (*Prinn and Fegley*, 1987). The ages, based on the decay of ^{53}Mn (half life 3.7 Myr), indicate that most carbonate assemblages in CI, CM and some other chondrites formed well after the formation of chondrules and almost certainly after the gaseous protoplanetary nebula had dissipated and after the parent body asteroids were assembled (*Hutcheon et al.*, 1998; *Brearley and Hutcheon*, 2002). This is all consistent with in-situ aqueous alteration following the melting of bulk ice by radioactive decay heating.

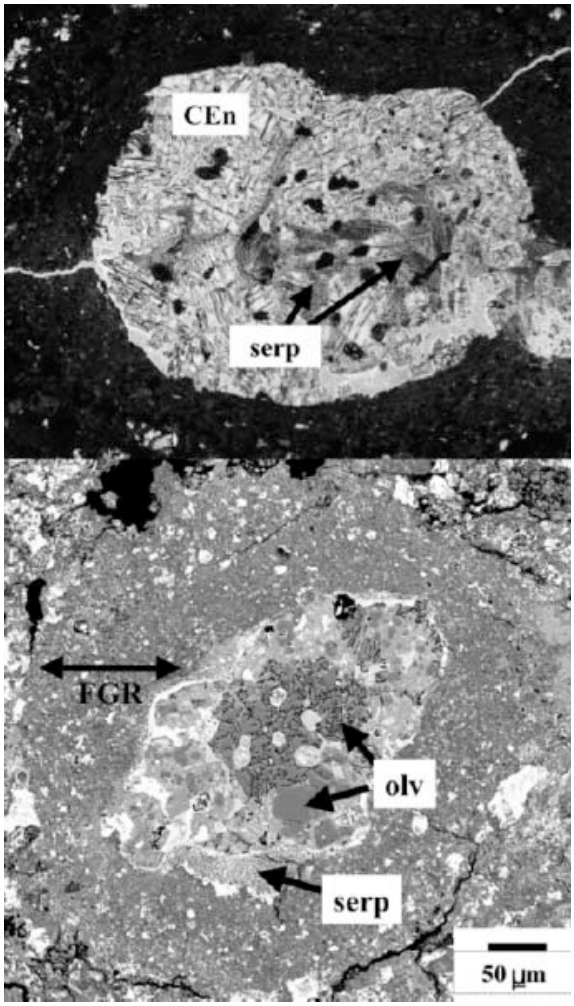

Fig. 3.— Images illustrating the replacement of chondrule phases by secondary serpentine in CM2 chondrites. (Top) Optical micrograph of a chondrule in Murchison, in which the primary chondrule glass has been replaced by serpentine (serp) probably during contact with liquid water. Image is approximately 2 mm across (from Brearley pers. comm, 2003). CEn is the high temperature (∼800 to 1000°C) phase clino-enstatite. Serpentine is a lower temperature (<400°C) phase and it is unlikely that these two phases formed during the same event. Serpentine is formed by secondary, low temperature alteration involving water. (Bottom) Backscattered electron (BSE) image of a chondrule in ALH81002, in which the primary olivine (olv) has been partially replaced by serpentine, again as a likely consequence of contact with liquid water. FGR is the fine-grained rim (from *Chizmadia and Brearley*, 2006).

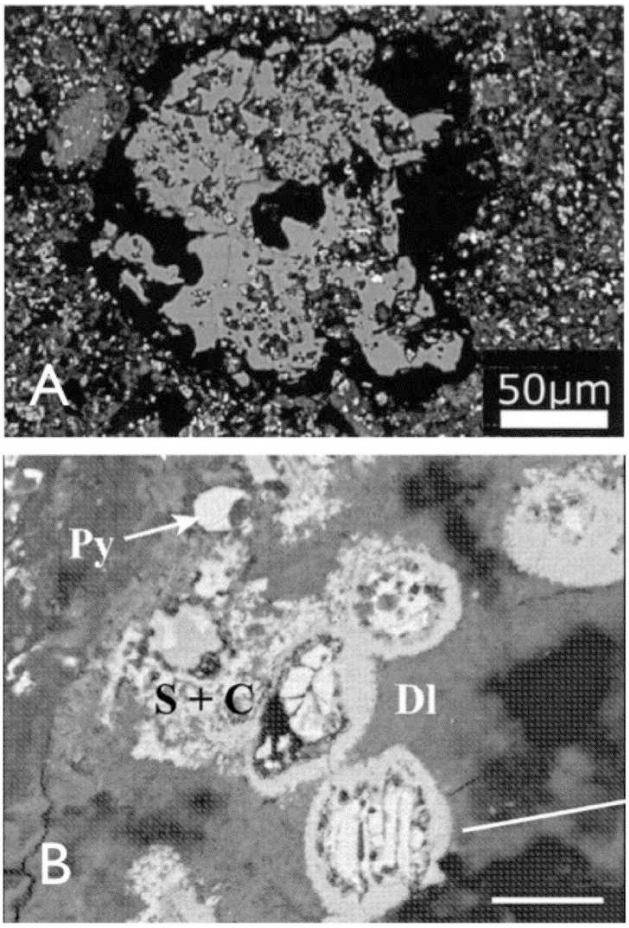

Fig. 4.— Back-scattered electron images of carbonate assemblages in carbonaceous chondrites. A) aragonite in the carbonaceous chondrite Tagish Lake (from *Nakamura et al.*, 2003) and B) a complex intergrowth of secondary phases in the CI-like chondrite, Y-86029 (from *Tonui et al.*, 2003). In panel B), S is sulphide, C is calcite, Dl is dolomite and Py is pyrrhotite (Fe_xS_{1-x}). The textural complexity seen in the Figure suggests formation in-situ from liquid water.

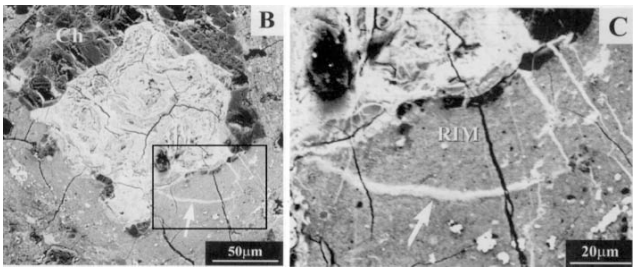

Fig. 5.— Back-scattered electron images of Fe-rich veins (arrows) protruding from an Fe-rich area of a chondrule (Ch) in the CM2 chondrite Murchison. The right-hand panel shows an enlargement of the boxed region on the left. The Fe-rich area of the chondrule was originally a metal grain that has been altered by contact with liquid water. The veins cut through the fine-grained rim and therefore must have formed after it, probably in conjunction with the aqueous alteration of the metal grain. From *Hanowski and Brearley* (2001).

2.3. Ordinary Chondrites

Although they are less oxidized and contain fewer volatiles than carbonaceous chondrites, ordinary chondrites also show several pieces of evidence indicating contact with an aqueous fluid.

First, phyllosilicates have been observed among the matrix materials in the unmetamorphosed (unheated) meteorites Semarkona and Bishunpur, indicating interaction with water (*Hutchison et al.*, 1987; *Alexander et al.*, 1989; *Grossman et al.*, 2000). Calcite, probably produced by aqueous alteration, has also been identified in Semarkona (*Hutchison et al.*, 1987).

Second, the outer portions of some chondrules show a "bleached" texture. Interaction with an aqueous fluid has resulted in the replacement of chondrule glass by phyllosilicates, while soluble elements such as Ca and Na have been removed (*Grossman et al.*, 2000; *Grossman and Brearley*, 2003).

Third, halite (NaCl) and sylvite (KCl) have been discovered in the ordinary chondrites Zag and Monahans (*Zolensky et al.*, 1998, 1999; *Bridges et al.*, 2004). The freezing-melting temperatures of the fluid inclusions in these salts are consistent with their having formed from a NaCl-H_2O brine at $<50°$. These are metamorphosed meteorites and the halite was formed after metamorphism. Moreover, ^{40}Ar-^{39}Ar and ^{129}I-^{129}Xe dates show that the halite crystals formed 4.0-4.2 Gyr ago (*Burgess et al.*, 2000).

Fourth, sulphur maps of ordinary chondrites and CO3 chondrites show that, with increasing degree of alteration, sulphur mobilizes into chondrules from matrix (*Grossman and Rubin*, 1999).

2.4. Interplanetary Dust Particles

Interplanetary dust particles (IDPs) are ejected from active comets and created by collisional grinding of asteroids (*Rietmeijer*, 1998). Some include a relic pre-Solar dust component. Many IDPs are chondritic in bulk composition and share many mineralogic similarities with chondritic meteorites (*Rietmeijer*, 1998). In addition, the dust measured from comet Halley by the Giotto Spacecraft was chondritic in composition (*Rietmeijer*, 1998). Some chondritic IDPs contain such secondary minerals as clays, serpentines, salts, carbonates, sulphides and oxides (*Brownlee*, 1978; *Rietmeijer*, 1991), again consistent with contact with liquid water.

3. ASTRONOMICAL EVIDENCE

Astronomically, water ice and hydrated minerals are detected primarily through their near infrared spectra. Ice has characteristic absorption bands due to overtones and combination frequencies in the thermally vibrating H_2O molecule. These occur in the near infrared at 1.5μm, 2.0μm and 3.0μm wavelength, with the 3μm band being the deepest but, observationally, most difficult to detect. Contamination of the water ice by absorbing matter (e.g., organics) can also reduce the depths of the characteristic bands, hiding water from spectroscopic detection. For example, laboratory experiments in which just a few percent (by weight) of absorbing matter are added to otherwise pure ice show that the band depths can be reduced to near invisibility in all but the highest quality spectra (*Clark and Lucey*, 1984).

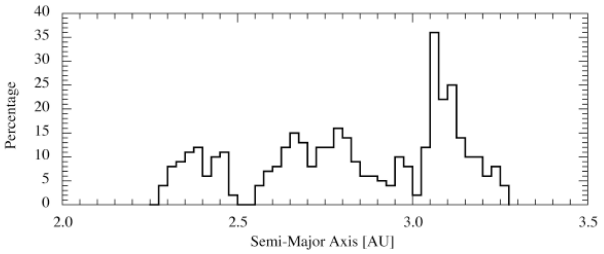

Fig. 6.— Fraction of asteroids (of all spectral types) showing the 0.7 μm band attributed to the $Fe^{2+} \rightarrow Fe^{3+}$ transition in hydrated material. Given that the 0.7 μm band is a proxy for OH, the figure may show the distribution of water across the main-belt. Replotted from *Carvano et al.* (2003).

Hydrated minerals show a characteristic band near 3 μm (due to structural OH and H_2O) but the shorter wavelength bands are normally absent or very weak. An alternative explanation in which the 3 μm band is due to OH radicals formed by implanted Solar wind protons may be compatible with some observations, but appears unable to account for the very deep features seen in phyllosilicates and many hydrated asteroids (*Starukhina*, 2001). Because of the practical difficulties of observing at 3 μm, there is interest in using correlated optical features as proxies. In particular, many clays show a band near 0.7 μm that has been attributed to an $Fe^{2+} \rightarrow Fe^{3+}$ charge transfer transition and which, empirically, is correlated with the harder-to-observe 3 μm band (*Vilas*, 1994). The fraction of the asteroids showing this feature varies with semi-major axis, being larger beyond $\sim$3 AU where the C-types (low albedo, neutral to slightly red) are dominant, but falling to zero in the D-type (dark and redder) Trojans beyond (Fig. 6).

3.1. Asteroids

Radiation equilibrium temperatures on the surfaces of main-belt asteroids are too high for the long-term stability of water ice. Therefore, little direct evidence exists for surface ice in the main-belt (however, see Ceres, below). On the other hand, spectral evidence for hydrated phases is very strong, particularly in the outer-belt (semi-major axis $>$2.5 AU) populations. Roughly half of the C-type asteroids, for instance, show spectral evidence for hydrated silicates in their 3 μm spectra (*Jones et al.*, 1990). Conversely, hydration features are generally not observed in the D-type and P-type asteroids that dominate the Jovian Trojan population at $\sim$5 AU. One interpretation is that the C-types were heated sufficiently for hydration reactions to occur but ice in the D- and P-types never reached the melting temperature, no hydration reactions took place, and so no hydrated materials are detected. Bulk ice could still be present in these more

distant objects (*Jones et al.*, 1990; *Jewitt and Luu*, 1990).

3.1.1. Ceres

Main-belt asteroid (1) Ceres has a mean diameter of 952±3.4 km, a density of ∼2077±36 kg m^{-3} and follows a nearly circular orbit (eccentricity e = 0.08) of semimajor axis 2.77 AU (*Thomas et al.*, 2005). The surface reflectivity is flat at visible wavelengths with an albedo near 0.11. Observations in the ultraviolet have shown tentative evidence for off-limb hydroxyl (OH) emission (*A'Hearn and Feldman*, 1992). Hydroxyl radicals could be produced by the photodissociation of water, and A'Hearn and Feldman suggested that their observation might be explained by the sublimation of water ice from polar regions of Ceres. Spectroscopic evidence for surface water ice is given by an absorption band at 3.06±0.02 μm and about 10% deep (Fig. 7, see *Lebofsky et al.*, 1981; *King et al.*, 1992; *Vernazza et al. 2005*). Observations in this wavelength region are very difficult and interpretations of the band vary based on details of the measured band shape. King et al. suggest that broadening of the band relative to pure ice could be due to NH_4 in the smectite clay mineral saponite. Vernazza et al. suggest instead a composite model incorporating crystalline water ice at 150 K and ion-irradiated asphaltite (a complex organic material).

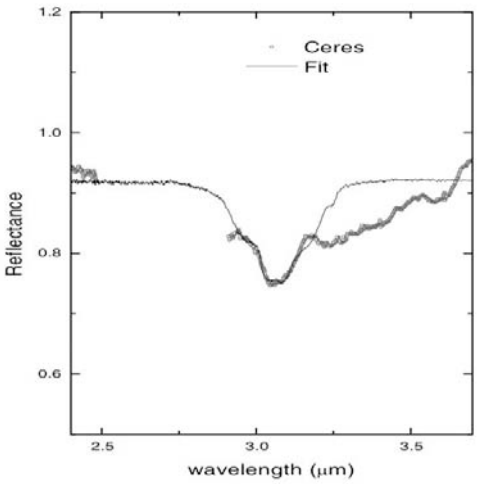

Fig. 7.— Spectrum of asteroid 1 Ceres showing the 3.06 μm absorption band attributed to crystalline water ice. The thin line is a model fit to the data. An additional absorber is required to match the data at wavelengths longer than 3.15 μm. From *Vernazza et al.* (2005)

Water ice on the surface of Ceres must have been recently emplaced because the sublimation lifetime at 2.8 AU is short (the sublimation rate is roughly 1 m yr^{-1}, if the ice is dirty and dark). On the other hand, although short-lived on the surface, *subsurface* ice on Ceres can be stabilized indefinitely at high latitudes by as little as ∼1m of overlying refractory mantle (*Fanale and Salvail*, 1989). We may surmise that water migrated to the surface from deeper down, perhaps in response to internal heating that has driven out volatiles (*Grimm and McSween*, 1989), perhaps creating fumarolic activity at the surface. Alternatively, ice could be excavated from beneath the mantle by impacts or deposited on the surface by impacting comets (as has been suggested to explain suspected polar ice deposits on the Moon and Mercury).

Thermal models (*McCord and Sotin*, 2005) show that, because of Ceres' considerable size, even heating by long-lived nuclei (K, Th, U) could lead to melting of deeply buried ice, followed by widespread hydration reactions with silicates in globally distributed hydrothermal systems. *Thomas et al.* (2005) report shape measurements that show that Ceres is rotationally relaxed with (weak) evidence for a non-uniform internal structure. Their models are consistent with water ice mantles containing ∼15% to 25% of the total mass: perhaps this is the ultimate source of the off-limb hydroxyl and the near-infrared absorption band.

3.1.2. Comets in the Asteroid Belt

Other evidence for ice in the main-belt comes from observations of the newly identified class of main-belt comets or "MBCs" (*Hsieh and Jewitt*, 2006). The best known example is asteroid (7968) 1996 N2 (also known as 133P/Elst-Pizarro or "EP") shown in Fig. 8. It displays a narrow, linear trail of dust morphologically reminiscent of the large-particle dust trails detected in the thermal infrared in the orbits of comets (*Sykes and Walker*, 1992). At first, the dust production was attributed to a recent impact and the likely parent of the impactor was identified as asteroid (427) Galene (*Toth*, 2000). The re-appearance of the trail in 2002 makes this explanation implausible and the dust is most likely ejected by sublimating ice (*Hsieh et al.*, 2004). Temporal evolution of the trail shows that the 2×3 km nucleus of EP ejects dust particles ∼10 μm in size at speeds ∼1.5 m s^{-1} over periods of months.

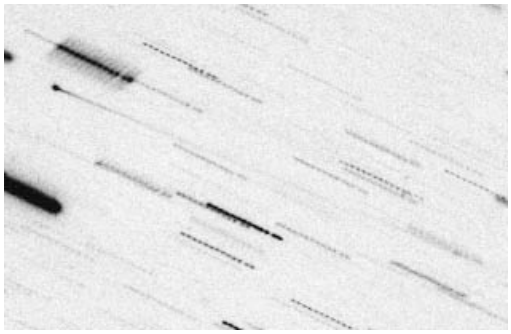

Fig. 8.— Composite R-band image of main-belt comet 133P/Elst-Pizarro from UT 2002 September 7 observations on the University of Hawaii 2.2 m telescope. The nucleus is at upper left with the dust trail extending across the entire field, down and to the right. The image is 2.5 by 3.5 arcmin in size, with north at the top and east to the left. This composite was produced by shifting and adding a set of short exposure images, causing fixed stars and galaxies to be streaked. Image from *Hsieh et al.* (2004).

Surface ice at the ∼3 AU heliocentric distance of EP has

a short lifetime to sublimation, meaning that the ice must have been recently emplaced in order for the activity to still be observed. *Hsieh et al.* (2004) considered two basic ideas concerning how these main-belt objects came to sublimate ice. The first possibility is that MBCs formed with the Jupiter family comets in the Kuiper belt and were transported by unknown processes to orbits that coincidentally appear asteroidal. However, published models of pure dynamical transport from the Kuiper belt fail to produce asteroid-like orbits (*Fernández et al.*, 2002). It is possible that model simplifications, including the neglect of gravitational deflections by the low-mass terrestrial planets and of rocket-forces due to asymmetric mass loss, might account for this failure. However, recent simulations including these extra forces do not produce MBCs with inclinations as low as that of 133P (*Fernández et al.*, 2002; *Levison et al.*, 2006).

The second idea is that MBCs formed in the main-belt, incorporating a substantial ice component. The observation that the orbital elements of EP are compatible with membership in the collisionally produced Themis family adds support to the conjecture that EP is a fragment from a larger, parent body that was shattered by impact. This cannot explain why the MBCs are outgassing now, however, since the age of the Themis family estimated from the dispersion of orbital elements of its members, is near 2 Gyr (*Marzari et al.*, 1995) and surface ice should have long-since sublimated away. Another trigger for outgassing must be invoked. One possibility is that a recent impact exposed buried ice, leading to sublimation that is modulated by seasonal variations in the insolation. The idea that the MBCs contain primordial ice is interesting in the context of the evidence for aqueous activity from the meteorites, discussed in Section 2.

3.2. Jovian Trojans

The Jovian Trojans co-orbit with the planet at 5.2 AU but librate around the L4 and L5 Lagrangian points, leading and trailing the planet by$\pm 60^\circ$ of longitude. The leading and following swarms together contain roughly 10^5 objects larger than kilometer scale (c.f. *Jewitt et al.*, 2004). The largest Trojan is (624) Hektor ($\sim 370 \times 195$ km).

The Jovian Trojan surfaces are located near the edge of the stability zone for water ice in the modern Solar system. They are outside the expected locations of the snow-line through most or all of the early evolution of the planetary system. If they formed in-situ, or at larger distances from the Sun, it is quite likely that the Trojans should be ice-rich bodies much like the nuclei of comets and the Kuiper belt objects.

Paradoxically, no direct evidence for water on the Trojans has been reported. The reflection spectra in the 0.4 μm to 2.5 μm wavelength range are generally featureless and slightly redder than the Sun (*Luu et al.*, 1994; *Dumas et al.*, 1998; *Cruikshank et al.*, 2001; *Emery and Brown*, 2004). The geometric albedos are low, with a mean value of 0.041 ± 0.002 (*Fernández et al.*, 2003). In these properties, the Trojans closely resemble the nuclei of comets. The data are consistent with the hypothesis that the Trojans, like the cometary nuclei, have ice-rich interiors hidden by a protective cap or "mantle" of refractory matter, probably left behind as a sublimation lag deposit. The low density of (617) Patroclus (800^{+200}_{-100} kg m^{-3}) also suggests a porous, ice-rich composition (*Marchis et al.*, 2006).

Might water ice be detectable on the Trojans? Clean (high albedo) water ice at 5 AU is cold enough to be stable against sublimation while dirty (absorbing, warmer) ice will sublimate away on cosmically short ($<10^4$ yr) timescales. Therefore, surface ice on Trojan asteroids that has been recently excavated by impacts might remain spectroscopically detectable until surface gardening (in which micrometeorite bombardment overturns the surface layers and mixes them with dirt) lowers the albedo, whereupon the ice would promptly sublimate. Spectroscopic surveys targeted to the smaller Trojans (on which collisions are more likely to provide large fractional resurfacing) might one day detect the ice.

The origin of the Trojans is presently unknown, with two distinct source locations under discussion. The Trojans could have formed locally and been trapped in the 1:1 resonance as the planet grew (*Chiang and Lithwick*, 2005). In this case, the compositions of the Jovian Trojans would reflect the $\sim$100 to $\sim$150 K temperature at 5 AU heliocentric distance and it would be permissible to think of the Trojans as surviving samples of the type material that formed Jupiter's high molecular weight core. Another possibility is that the Trojans formed at some remote location, possibly the Kuiper belt, and were then scattered and captured during a chaotic phase in the Solar system (*Morbidelli et al.*, 2005). In this case, the Trojans would be captured Kuiper belt objects, presumably with initial ice contents equal to those of the comets. In either case, the volatile-rich interiors of the Trojans would be protected from insolation by a lag deposit consisting of refractory matter. It is interesting that the Trojans and the cometary nuclei are so similar in the color-albedo plane. This fact is not proof that Trojans are comets, but it is consistent with this inference. On the other hand, the Trojans are less red (*Jewitt*, 2002) and darker (*Fernández et al.*, 2003) than the KBOs. If they were captured from the Kuiper belt then unspecified evolutionary processes must have acted to both darken their surfaces and remove very red material.

One meteorite known as Tagish Lake shows spectral similarities to D-type (and P-type) asteroids (Fig. 9; *Hiroi et al.*, 2001; *Hiroi and Hasegawa*, 2003) and so is a candidate for the type of material which might make up the Trojans. Similarities include a low albedo (a few % at visual wavelengths) and reddish color, with a featureless optical to near infrared reflection spectrum. Tagish Lake is an anomalous carbonaceous chondrite which was observed to fall and immediately recovered from frozen ground in Canada in 1999. It shows abundant evidence for aqueous alteration in the form of Mg-Fe carbonates and phyllosilicates (*Nakamura*

et al., 2003).

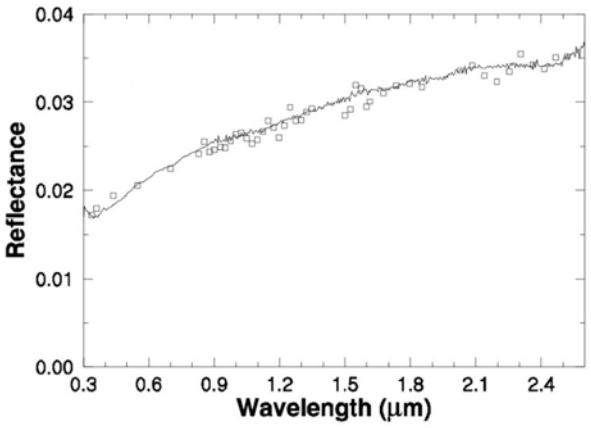

Fig. 9.— A comparison of the reflectance spectra of Tagish Lake (line) with the D-type asteroid (368) Haidea (points). Figure courtesy of *Hiroi et al.* (2001).

3.3. Cometary Nuclei

Water is well known in the nuclei of comets. It sublimates inside a critical distance near 5 AU or 6 AU to produce the distinctive coma (gravitationally unbound atmosphere) and tails that observationally define comets. The thermal response of water ice to the varying insolation on a comet moving in an eccentric orbit about the Sun formed the basis of *Whipple's* (1950) classic comet model. Whipple thought that water might carry about 50% of the nucleus mass. Recent estimates based on long wavelength (infrared and submillimeter) radiation show that water is less important, perhaps carrying only 20% to 30% of the mass in typical nuclei (*Sykes et al.*, 1986).

The water ice in comets appears to have condensed at temperatures in the range 25 to 50 K. Several lines of evidence lead to this temperature range, which (in the present epoch) is characteristic of heliocentric distances beyond Neptune. First, comets are sources of CO, with production rates relative to water in the $\sim$1% to $\sim$20% range. The CO molecule is highly volatile and difficult to trap at temperatures much above 50 K. Laboratory experiments in which CO is trapped in amorphous ice suggest accretion temperatures near 25 K (*Notesco and Bar-Nun*, 2005). The nuclear spin temperature, which is thought to be set when the water molecule forms, is near 30 K in those comets for which it has been accurately measured. Measurements of the D/H ratio in H_2O and HCN in comet C/Hale-Bopp are compatible with ion-molecule reactions at 30 ± 10 K, probably in the collapsing cloud that formed the Solar system (*Meier et al.*, 1998b). Water ice formed at temperatures below $\sim$110 K is thermodynamically stable in the amorphous (disordered) state. The ice in two comets (C/Hale-Bopp, *Davies et al.*, 1997 and C/2002 T7 (LINEAR), *Kawakita et al.*, 2004) has indeed been inferred to be amorphous, based on the absence of the 1.65 μm feature of crystalline ice. However, since water ice is rarely detected in comets, we do not know from observations whether the ice in comets is generally amorphous. Models assuming abundant amorphous ice have been constructed to take advantage of the exothermic transition to the crystalline phase in order to power cometary activity at distances slightly beyond the critical distance for sublimation in radiative equilibrium with the Sun (*Prialnik*, 1992; *Prialnik et al.*, 2005).

Most recently, thermal infrared observations of the ejecta produced by the impact of NASA's Deep Impact spacecraft into the nucleus of P/Tempel 1 have shown tentative evidence for hydrated minerals (*Lisse et al.*, 2006). If confirmed (for instance by samples returned in NASA's Stardust mission) this detection would seem to require that the hydrated minerals be formed in the gas phase before incorporation into the nucleus, since it is hard to imagine how this small cometary nucleus could have been hot enough to sustain liquid water and yet retain substantial quantities of volatile ices such as CO.

3.4. Kuiper Belt Objects and Centaurs

As with the Trojan asteroids and cometary nuclei, the optical reflection spectra of most KBOs and Centaurs rise linearly with wavelength and are spectrally featureless. The proportion showing identifiable absorption bands is, however, higher and this presumably reflects the lower rates of sublimation at the greater distances of these objects. The main problem in the study of KBOs and Centaurs is a practical one: most are very faint, technically challenging astronomical targets.

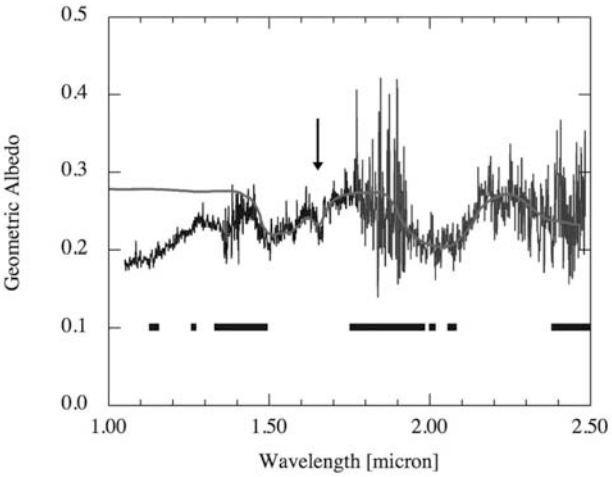

Fig. 10.— Reflection spectrum of KBO (50000) Quaoar in the near infrared, showing broad bands due to water at 1.5 μm and 2.0 μm, and a narrower feature at 1.65 μm that is specifically due to crystalline water ice (arrow). The smooth line is a water ice spectrum that is over-plotted (but not fitted) to the astronomical data. Horizontal bars mark wavelengths at which the Earth's atmosphere absorbs. From *Jewitt and Luu* (2004).

Figure 10 shows the 1.5 μm and 2.0 μm bands of water ice in the reflection spectrum of $\sim$1200 km diameter KBO

(50000) Quaoar (*Jewitt and Luu*, 2004). A third band at 1.65 μm is diagnostic of the presence of crystalline (not amorphous) water ice. This result is curious, given that Quaoar is at 43 AU and the surface temperature is near 50 K or less: ice would be indefinitely stable in the amorphous form at this temperature. The inevitable conclusion is that the ice exposed on the surface of Quaoar, though now cold, has been heated above the critical temperature ($\sim$110 K) for transformation to the crystalline form. Furthermore, the ice on Quaoar (and all other airless bodies) is exposed to continual bombardment by energetic photons from the Sun, and particles from the Solar wind and from interstellar space (the cosmic rays). These energetic photons and particles are capable of breaking the bonds in crystalline ice, converting it back to a disordered, amorphous state on a timescale that may be as short as 10^6 to 10^7 yrs (*Mastrapa et al.*, 2005). Thus, we may also conclude that the ice surface on Quaoar is young. How could this be?

The bulk of the ice inside Quaoar could have been heated above the amorphous to crystalline phase transition temperature by internal processes. Quaoar is large and radiogenic heat is capable of raising the internal temperatures substantially above the low values on the surface and in the nebula at 43 AU (see Section 5). This bulk crystalline material must be replenished at the surface in order to avoid reamorphization. One mechanism is micrometeorite "gardening", in which continual bombardment overturns the surface layers, dredging up fresh material and burying the instantaneous surface layer. Given that near infrared photons probe to depths of only a few millimeters, the gardening rate only needs to be large compared to a few millimeters per 10^6 or 10^7 yr. We know essentially nothing about the micrometeorite flux in the Kuiper belt, but it seems reasonable that such a low rate could be sustained. Another mechanism is simple eruption of crystalline ice onto the surface via the action of cryovolcanism. In the context of the Kuiper belt, cryovolcanism need not involve the eruption of liquid water, but could be as simple as the leakage of a volatile gas, perhaps CO mobilized by heating at great depth, with the entrainment of crystalline ice particles into the flow. It is worth noting that Quaoar is not alone in showing crystalline water ice: several satellites of Uranus as well as Pluto's satellite Charon also have crystalline ice on the surfaces. Are they all cryovolcanically active? Intuition says this is unlikely but recent observations of Saturn's satellite Enceladus show that it is outgassing and populating the E-ring with dust particles. Enceladus has a source of energy (tidal heating) that is unavailable to KBOs, but it is also much smaller (500 km diameter, compared to Quaoar's 1200 km) and faster to cool.

4. ISOTOPIC EVIDENCE

4.1. Hydrogen

Most models indicate that the Earth formed inside the snow line and so formed dry (see Fig. 1). However, the Earth is not dry (the mass of the oceans is $\sim 3\times10^{-4}$ $M_\oplus$), raising the question of how it acquired its water. Likely sources include ice-rich bodies accreted outside the snowline and transported inwards to impact the Earth after its formation, providing a late-stage volatile veneer (*Owen and Bar-Nun*, 1995). These could be bona-fide comets from the outer regions or asteroids from the main-belt. A potentially important constraint on the source population can be set from measurements of the deuterium/hydrogen (D/H) ratio. The standard mean ocean water (SMOW) value is D/H = 1.6×10^{-4}, while measurements in comets give a value about twice as large, namely D/H $\sim 3.3\times10^{-4}$ (see *Meier et al.*, 1998a and *Meier and Owen*, 1999 for descriptions). It is tempting to conclude on this basis that the comets cannot be the dominant suppliers of Earth's water but this conclusion is probably premature. First, the formal significance of the difference between D/H in comets and in SMOW is marginal (and also difficult to judge, given that systematic errors rival statistical ones in the remote determination of D/H). Second, the measured comets are Halley-family or long-period objects, dynamically unlike the Jupiter family comets (JFCs) that may have dominated the volatile delivery to Earth. The JFCs and long-period comets may originate from different regions within the protoplanetary disk and at different temperatures (although this is itself far from certain). If the measured comets have D/H ratios that are not representative of the dominant impactors then objections based on isotopic differences with SMOW would disappear. Unfortunately, most comets are too faint for astronomical determinations of D/H and in-situ measurements from spacecraft will be needed to acquire a large, dynamically diverse sample.

Other possible sources include ice-rich "asteroids" from the outer parts of the main-belt. This source is appealing because some measurements of D/H in hydrated meteorites are close to the SMOW value. Furthermore, some dynamical models purport to show that the main-belt could also supply a sufficient mass of water to Earth to explain the oceans (*Morbidelli et al.*, 2000). Unfortunately, the mechanism by which the main-belt was cleared and the timing of this event relative to the formation of Earth remain uncertain. Also, noble gas abundance patterns on the Earth are unlike those in the meteorites and it is not obvious how this difference can be explained if these gases were delivered, with water, from the asteroid belt. Noble gas abundances in comets are unmeasured. Future measurements of D/H in water from main belt comets (Section 3.1.2) will be of great interest in this regard.

4.2. Oxygen

Measurements of the $^{16}O/^{17}O$ and $^{16}O/^{18}O$ ratios in primitive meteorites show mass-independent variations that are distinct from the mass-dependent fractionation produced from chemical reactions. Mass-independent variations may be caused by the mixing of ^{16}O-rich with ^{16}O-poor material in the asteroid-belt source region where the meteorite parents formed (*Krot et al.*, 2005). Optical

depth effects in the protoplanetary nebula, coupled with the freeze-out of water, could be responsible (*Krot et al.*, 2005). Gas phase $C^{16}O$ would be optically thick to ultraviolet photons in much of the young nebula and thus immune to photodissociation. The more rare isotopomers $C^{17}O$ and $C^{18}O$ could be optically thin, especially above the disk mid-plane and at large heliocentric distances. Atoms of ^{17}O and ^{18}O produced by dissociation beyond the snow line would be picked up by water molecules and soon trapped as ice. In this way, ice-bearing solids would become progressively depleted in ^{16}O relative to the gas (which is ^{16}O enhanced), by an amount that depends upon the disk gas mass, the heliocentric distance and the degree of mixing upwards from the mid-plane (*Lyons and Young*, 2005). Inward drift of icy planetesimals across the snow line leading to their sublimation would return ^{16}O-poor water to the gas phase. One feature of this model is that it requires a flux of UV-photons comparable to that expected from an O or B-type star located within $\sim$1 pc of the Sun (*Lyons and Young*, 2005). If this is the correct interpretation of the mass-independent oxygen isotope variations then it provides evidence that the Sun was part of a stellar cluster (since O and B-type stars are rare, and on-average found at much larger distances).

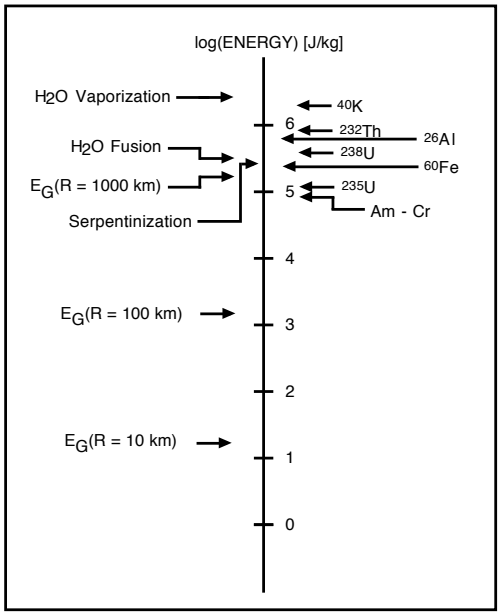

Fig. 11.— Energy per unit mass for processes relevant to the thermal evolution of small bodies. Isotope symbols show the time-integrated energy production from the given element divided by the total mass of the small body, computed assuming cosmic initial abundances of the elements. Energies for the amorphous - crystalline (Am - Cr) phase transition and for H_2O fusion and vaporization are per unit mass of ice, while that for serpentinization is per unit mass of serpentine (as in Section 4). E_G is the gravitational binding energy per unit mass, given for a homogeneous sphere by E_G = 3 G M / (5 R) and computed assuming a density of 1000 kg m^{-3}. Another heat source due to electromagnetic induction in the magnetic field of the young sun has been discussed in the context of asteroids (c.f. *McSween et al.*, 2002), but is of uncertain magnitude, declines precipitously with heliocentric distance and is not plotted here.

5. THERMAL EVOLUTION OF SMALL BODIES

5.1. Analytical Considerations

Thermal evolution in the presence of ice is an exciting topic that promises to throw much light on the interrelations between comets and asteroids (*Jewitt*, 2005) and on their water and volatile histories (*Prialnik et al.*, 2005). Minimal requirements for the stability of liquid water include temperatures *and* pressures above the triple-point values 273 K and 600 N m^{-2}, respectively. Central hydrostatic pressure in a spherical body of density ρ and radius r is $P_c \sim 2\pi/3$ G ρ^2 r^2. With ρ = 10^3 kg m^{-3}, $P_c \geq$ 600 N m^{-2} for $r \geq$ 2 km. Smaller bodies can never sustain the triple-point pressure unless they are strong (which, in the context of prevailing formation scenarios seems unlikely). In larger bodies, whether liquid water can be stable at depth depends mainly on the existence of heat sources adequate to raise the temperatures above the triple point value. Gravitational binding energy is too small to melt or vaporize ice in any but the largest bodies considered in this chapter (see Fig. 11). Instead, in the asteroid belt the dominant heat source was likely ^{26}Al (*Lee et al.*, 1976; *MacPherson et al.*, 1995). The influence of ^{26}Al depends on the size of the body, on the mechanisms of heat loss, and on the time elapsed between the explosion of the ^{26}Al-producing supernova and its incorporation into the growing body (*Ghosh et al.*, 2003).

A lower limit to the rate of loss of heat from a body of radius r is set by thermal conduction. The conduction cooling time is

$$\tau_c \sim \frac{r^2}{\kappa} \quad (1)$$

where κ is the thermal diffusivity given by $\kappa = k/(\rho c_p)$, k = thermal conductivity, ρ = density and c_p = specific heat capacity. Common non-porous solids have $\kappa \sim 10^{-6}$ m^2 s^{-1} while porosity may reduce this by a factor of $\sim$10. The heat released by ^{26}Al can only be effective when $\tau_c >> \tau$, which corresponds to $r_c >> (\kappa\tau)^{1/2}$, where τ is the time constant for the decay of ^{26}Al. Substituting κ = 10^{-6} m^2 s^{-1} and $\tau \sim$ 1 Myr, we obtain $r_c >>$ 5 km for the critical size above which strong thermal effects are expected. Bodies much larger than a few kilometers in size, then, are candidates for having central hydrostatic pressures high enough, and cooling times long enough, to nurture liquid water.

A crude calculation of the effect of radioactive heating may be obtained by considering a body of radius r and initial temperature T_0, represented by a unique (average) internal temperature $T(t)$ as a function of time t. Assuming a radioactive source of initial mass fraction X_0 and decay en-

ergy per unit mass of rock H, the energy balance equation for the body is

$$c_p \frac{dT(t)}{dt} = X_0 H \tau^{-1} e^{-t/\tau} - \frac{3kT(t)}{\rho r^2}, \qquad (2)$$

where the second term on the RHS of Equation (2) is the cooling flux (*Merk and Prialnik*, 2003). Assuming constant, average values c_p and k, this equation can be solved analytically to obtain the time t_1 required to reach the melting temperature $T(t_1) = T_m = 273\ K$, and the amount of radioactive material still available $X_1 = X_0 e^{-t_1/\tau}$,

$$T(t) = T_0 e^{-at} + \frac{b}{a\tau - 1}\left[e^{-t/\tau} - e^{-at}\right], \qquad (3)$$

where

$$a(r) = \frac{3k}{\rho c_p r^2} = \frac{3\kappa}{r^2},\ b = \frac{X_0 H}{c_p}\ . \qquad (4)$$

When the melting temperature is reached, the heat released is absorbed by the melting ice and the temperature does not rise any longer. Thus, energy balance for times later than t_1 reads

$$H_m \dot{Y}_m = X_1 H \tau^{-1} e^{-t/\tau} - \frac{3kT_m}{\rho r^2}, \qquad (5)$$

where H_m=latent heat of melting, $Y_m(t)$ is the volume fraction of liquid water, and t is set to zero at the onset of melting. The solution

$$Y_m(t) = H_m^{-1}\left[X_1 H(1 - e^{-t/\tau}) - \frac{3kT_m}{\rho r^2} t\right] \qquad (6)$$

rises to a maximum and declines to zero. The time span for which $Y_m > 0$, that is, for which liquid water is present, can be easily estimated. (Equation (6) gives a strong upper limit to the duration of the liquid phase, since energy transport by convection in liquid water will dominate the cooling flux and suppress temperatures much faster than conduction). Representative results for the time required to reach the melting temperature, the maximal volume fraction of water attained and the duration of the liquid phase are given in Fig. 12, considering the effect of ^{26}Al and of the most potent long-lived radioactive species, ^{40}K. The values of constants assumed are κ = 10^{-6} m^2 s^{-1} (as above) and c_p = 10^3 J kg^{-1}; the radioactive abundances assumed correspond to a 1:1 mass ratio of ice to dust. A time delay of 2 Myr was assumed in the case of ^{26}Al to account for the imperfect trapping of this short-lived isotope.

These simple models show that, while small bodies - a few kilometers in size - are completely unaffected by ^{40}K, bodies of a few hundred kilometers radius may have retained liquid water in their interiors up to the present. Significant amounts of liquid water may be expected in smaller bodies, heated by ^{26}Al, only for radii above $\sim$ 20 km; the water is expected to refreeze on a time scale of $\sim$ 20 Myr.

5.2. Numerical Modeling - Icy Bodies (Comets)

Obviously, all these quantities are only rough estimates based on a crude analytical treatment. Somewhat egregiously, we have allowed cooling only by conduction when, in fact, solid state convection may dominate the cooling rate long before the melting temperature is reached (*Czechowski and Leliwa-Kopystynski*, 2002). Countering this, water may add new sources of heat. First, if the accreted ice is initially amorphous (unlikely in the hot inner Solar system but possible in the cold Kuiper Belt) then the energy of the amorphous to crystalline phase change is available. This is $\sim 9 \times 10^4$ J kg^{-1}, sufficient to drive a wave of crystallization through the icy portions of any body. Second, if the liquid state is reached, powerful serpentinization reactions may come to dominate the heat production, at least locally (section 5.3).

On the other hand, numerical models that treat thermal evolution in detail necessarily have a large number of free parameters. Thus, usually, models focus on the effect of one parameter or characteristic and the results obtained may only be taken to indicate trends of behavior. For example, *Haruyama et al.* (1993) investigate the potential effect of a very small thermal conductivity on the crystallization of amorphous ice due to radioactive heating in a H_2O ice and dust body. Not surprisingly, they find that for very low conductivities, a runaway increase in the internal temperature occurs and most of the ice crystallizes, while for sufficiently high conductivities, the initially amorphous ice may be almost entirely preserved. A similar study by *Yabushita* (1993) investigates the possibility of melting and formation of organic chemicals due to radioactive heating and finds that a very low diffusivity allows for melting in the interior of relatively large icy bodies ($r \gtrsim 200$ km). However, these studies neglect heat transport by vapor flow through the porous nucleus and the possibility of internal sublimation or recondensation. Vapor flow is taken into account by *Prialnik and Podolak* (1995), who consider radioactive heating in porous nuclei, allowing for trapped CO gas in the amorphous ice, which is released upon crystallization. A large variety of results are obtained by varying the basic parameters: porosity, radius, thermal conductivity and ^{26}Al content. Porosity and heat advection by the flowing gas are shown to affect the thermal evolution significantly. Thus, only for a very low porosity and very low conductivity is it possible to obtain an extended liquid core for a considerable period of time. However, this study does not consider ices of volatiles besides H_2O in the initial composition. These are considered by *Choi et al.* (2002), who show that ices of highly volatile species have a considerable effect on the early crystallization pattern of H_2O ice induced by radioactive heating, both by absorbing and by releasing latent heat. Thus, they find that even large bodies ($r \sim 50$ km) may retain the ice in amorphous form, despite radioactive heating (even including some ^{26}Al). However, the effect of advection by volatile flow is maximized in their study by assuming a very high permeability.

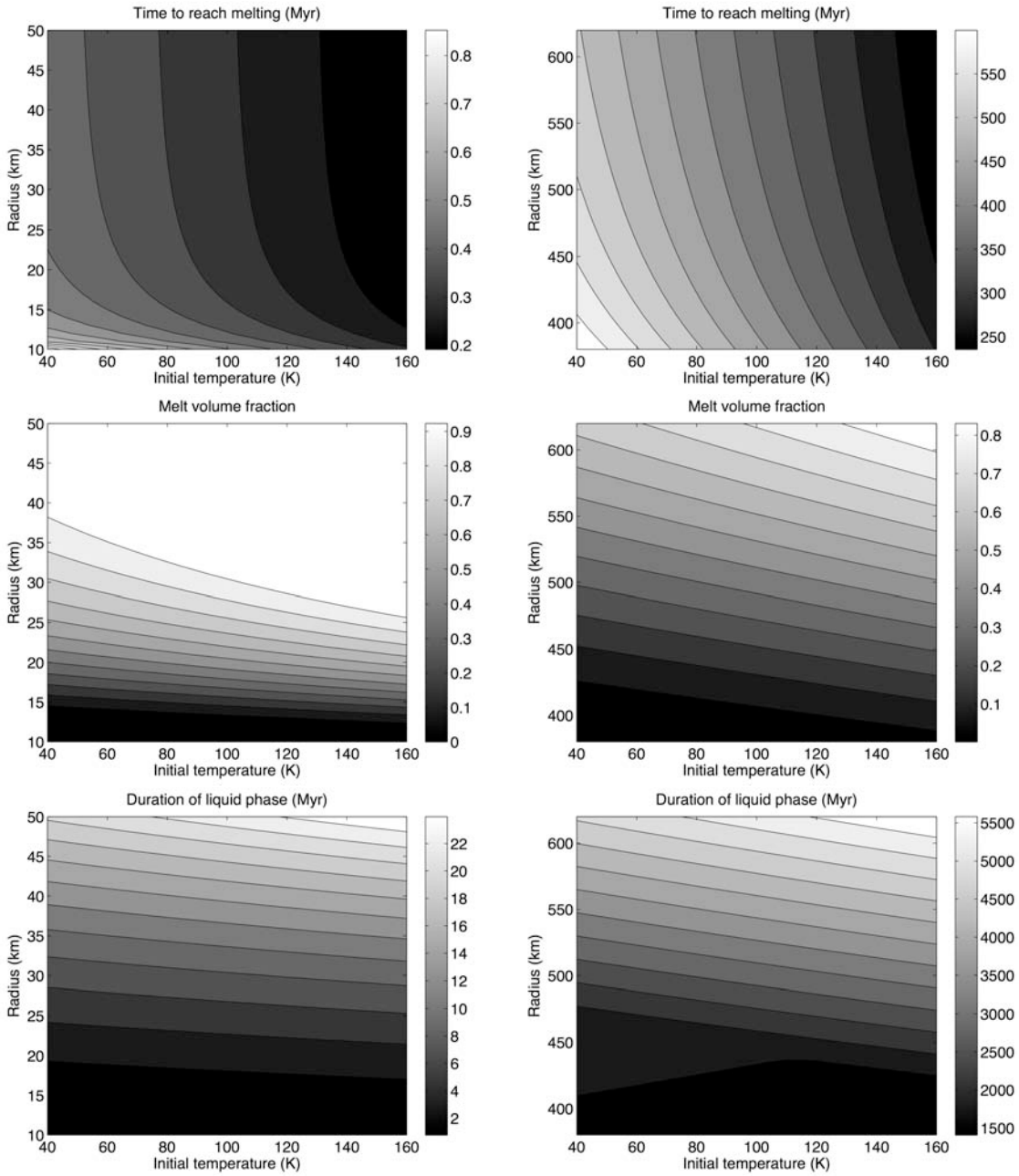

Fig. 12.— Models for the thermal evolution of small bodies heated by radioactive decay as a function of their radius and initial temperature assuming a 1:1 ice: rock mass ratio. Left and right columns show models heated by the decay of ^{26}Al and ^{40}K, respectively (see text). At the top is shown the time to reach the water ice melting point, in the middle is the fractional melt volume while at the bottom is the duration of the liquid phase.

Despite the non-uniqueness inherent in presently available models, it is clear that heating by ^{26}Al is potentially so strong that even silicates could have been melted in small asteroids if they formed early enough to trap this isotope (e.g., *Herndon and Herndon*, 1977; *Grimm and McSween*, 1993). Conversely, delayed aggregation into large bodies would minimize the thermal impact of ^{26}Al: after 10 half-lives ($\sim$7 Myr) the available heat from ^{26}Al is reduced by a factor of 2×10^4 and can be ignored. In bodies that formed quickly enough relative to the ^{26}Al decay, radioactive heating may drive melting in the central region of a relatively small icy body, the question remains of the consequences of a liquid core, considering that water is much denser than ice. So far, this problem has not been considered in detailed numerical simulations - largely due to the fact that structural parameters of cometary material are poorly known - and not much progress has been made beyond the early analytical work of *Wallis* (1980), who treated a vapor-droplet mixture within an icy shell.

The formation timescale, t_f, is crucially important in determining the thermal evolution of a body. For bodies of a given size, t_f varies in inverse proportion to the surface density in the accretion disk of the Sun (the latter may have varied as $\propto$ R$^{-3/2}$) and in proportion to the Keplerian orbit period ($\propto$ R$^{3/2}$). When multiplied together, these give $t_f \propto$ R^3. All else being equal, an object taking 2 Myr to accrete in the main-belt at 2.5 AU would take $\sim$20 Myr at the 5 AU distance of the Jovian Trojans. Twenty million years corresponds to about 28 half-lives of ^{26}Al, precluding any heating from this source in the Trojans whereas heating of the main-belt objects could be strong. The strong heliocentric distance dependence of the growth time is consistent with a large radial gradient in their hydration properties across rather modest radial distance differences (*Grimm and McSween*, 1993). Taken out to the Kuiper belt (30 AU and beyond) the formation times predicted by this simple scaling law approach the age of the Solar system, and are unreasonable. Detailed models of Kuiper belt object accretion show that such objects can form on much more reasonable (10 Myr - 100 Myr) timescales provided very low velocity dispersions are maintained (*Kenyon*, 2002) but reinforce the point that the KBOs are probably much less heated by trapped ^{26}Al or other short-lived nuclei compared to inner-disk objects of comparable size. The primitive meteorites, especially those which are hydrated, show that early melting of silicates was not a universal fate even in the asteroid belt, and in the parents of these meteorites we seek to examine the effects of heating on buried water ice. We should bear in mind, however, that heating by ^{26}Al may well take place during the accretion process itself; moreover, the accretion rate is not linear in time. Thus, the core of an accreting body may be significantly heated before the body reaches its final size long after the decay of ^{26}Al. The effect of combined growth and internal heating by ^{26}Al decay was investigated by *Merk and Prialnik* (2003) for an amorphous ice and dust composition, without other volatiles. They found that while it still remains true that small objects remain almost unaffected by radioactive heating, the effect on larger bodies is not linear with size. There is an intermediate size range (around 25 km), where the melt fraction and duration of liquid water are maximal, and this range depends strongly on formation distance (ambient temperature). The corresponding calculation for an asteroid is by *Ghosh et al.* (2003).

5.3. Small Bodies and Serpentinization

If the water triple point is reached, exothermic hydration reactions with rock (so-called "serpentinization" reactions) can generate their own heat. The heat produced varies depending on the specific hydration reaction under consideration. For the (idealized) serpentine-producing reaction

$$Mg_2SiO_4 + MgSiO_3 + 2H_2O \leftrightarrows Mg_3Si_2O_5(OH)_4 \quad (7)$$

the energy released per unit mass of serpentine produced is 2.4×10^5 J kg^{-1} (*Grimm and McSween*, 1989; *Cohen and Coker*, 2000, see also *Jakosky and Shock*, 1998 for energetics of other reactions). In this reaction, two moles (about 36 g) of water react with rock to produce one mole (about 276 g) of serpentine. Enough energy is produced to melt about 40 moles (730 g) of water ice (the latent heat of fusion is 3.3×10^5 J kg^{-1}). Therefore, depending on the details of the heat transport within the parent body, there is the possibility for a thermal runaway in which heat from serpentinization in a localized region of the asteroid triggers the melting of ice throughout the body. An everyday example of this type of chemical energy release is commercial concrete which, when mixed with water, liberates heat. A natural, terrestrial example may have been found in the mid-Atlantic, Lost City hydrothermal complex (Fig. 13). Lost City is located far from the mid-ocean ridge heat source and emits fluids with distinctive chemical properties different from those at the mid-ocean ridge, suggesting the action of serpentinization reactions (*Kelley et al.*, 2001: note that this interpretation is contested by *Allen and Seyfried*, (2004) on geochemical grounds). Lost City has been active for 30,000 yr, produces a few MW of power (corresponding to serpentinization at a rate $\sim$10 kg s^{-1}) and has enough reactants to continue for $\sim10^6$ yr (*Fruh-Green et al.*, 2003).

Models of runaway serpentinization in main-belt asteroids have been computed by different groups, leading to some spectacular, if arguable, conclusions. In these models, ice melting occurs first as a result of radioactive decay heating by short-lived isotopes. Serpentinization then releases a tremendous amount of heat which dominates the subsequent thermal evolution. Such heating may be moderated in reality by the rate at which water can be introduced to reaction sites or by efficient heat loss due to hydrothermal convection. Bodies of asteroidal porosity must be a few hundred kilometers in diameter, however, to initiate hydrothermal convection (*Grimm and McSween*, 1989; *Young et al.*, 2003). If heating is too rapid or hydrothermal circulation does not otherwise develop, high steam pressures could

cause parent-body rupture under conditions of low permeability (*Grimm and McSween*, 1989; *Wilson et al.*, 1999).

Fig. 13.— Carbonate chimneys at the Lost City field rise up to 60 m above the surrounding terrain and heat sea water to 40° to 75°C above ambient. They may be entirely powered by serpentinization. Figure courtesy of University of Washington.

Bodies which are too small, or those which form too late, are unable to trap much ^{26}Al and never attain temperatures sufficient to melt ice. In these, the serpentinization reactions are never triggered, except perhaps sporadically by heating events caused by large impacts (*Abramov and Kring*, 2004). For this reason, we expect that the effects of serpentinization reactions in the KBOs are also much diminished, except perhaps in the larger objects where longer-lived unstable nuclei (^{40}K, ^{235}U, ^{238}U and ^{232}Th) might drive water above the melting temperature, at least locally, at later times (*Busarev et al.*, 2003). Serpentinization also releases hydrogen which, following Fischer-Tropsch type reactions, could lead to the production of methane (CH_4) from CO or CO_2. Methane is known on the surface of Pluto and has been recently detected on other large Kuiper belt objects (*Brown et al.*, 2005) but is not expected to have been abundant in the Solar nebula from which these objects formed (*Prinn and Fegley*, 1981). Serpentinization could be the ultimate source.

Acknowledgements. We thank the anonymous referee for a review and Audrey Delsanti, Henry Hsieh, Jane Luu, Toby Owen, Bin Yang for helpful comments. This work was supported by NASA grant NNG05GF76G to DJ, by the NASA Astrobiology Institute under Cooperative Agreement No. NNA04CC08A issued through the Office of Space Science, by NASA cosmochemistry grant NAG5-11591 to Klaus Keil, by Israel Science Foundation grant 942/04 to DP and by NASA's Outer Planets Research grant NNG05GG60G to RG.

REFERENCES

A'Hearn M. and Feldman P. (1992) *Icarus, 98,* 54-60.

Abramov O. and Kring D. (2004) *J. Geophys. Res. (Planets), 109,* E10007.

Allen D. E. and Seyfried W. E. (2004) *Geochim. Cosmochim. Acta, 68,* 1347-1354.

Brearley A. J. (2003) In *Treatise on Geochemistry* (H. D. Holland and K. K. Turekian, eds.). pp. 247-268. Elsevier, Oxford.

Brearley A. J. and Hutcheon I. D. (2002) *Meteorit. Planet. Sci., 37,* Supplement, A23,

Bridges J. C., Banks D. A., Smith M., and Grady M. M. (2004) *Meteorit. Planet. Sci., 39,* 657-666.

Brown M. E., Trujillo C. A., and Rabinowitz D. L. (2005) *Astrophys. J., 635,* L97-100.

Browning L. B., McSween H. Y. and Zolensky M. E. (1996) *Geochimica et Cosmochimica Acta, 60,* 14 2621-2633.

Browlee D. E. (1978) In *Protostars and Planets* (T. Gehrels, ed.) pp. 134-150. Univ. of Arizona, Tucson.

Burgess R., Whitby J. A., Turner G., Gilmour J. D. and Bridges J. C. (2000) *Lunar and Planetary Science Conference XXXI* abstract No. 1330.

Busarev V. V., Dorofeeva V. A., and Makalkin A. B. (2003) *Earth, Moon and Planets, 92,* 345-375.

Carvano J. M., Mothé-Diniz T., and Lazzaro D. (2003) *Icarus, 161,* 356-382.

Chiang E. I. and Lithwick Y. (2005) *Astrophys. J., 628,* 520-532.

Chizmadia L. and Brearley A. (2006) In prep.

Choi Y.-J., Cohen M., Merk R., and Prialnik D. (2002) *Icarus, 160,* 300-312.

Ciesla F. J., Lauretta D. S., Cohen B. A., and Hood L. L. 2003, *Science, 299,* 549-552.

Ciesla F. J. and Cuzzi J. (2006) *Icarus,* in press.

Clark R. N. and Lucey P. G. (1984) *J. Geophys. Res., 89,* 6341-6348.

Clayton R. N. (1993) *Ann. Rev. of Earth Science, 21,* 115-149.

Clayton R. N. (1999) *Geochimica et Cosmochimica Acta, 63,* 2089-2104.

Clayton R. N., Mayeda T. K. and Onuma N. (1976) *Earth and Planetary Science, 30,* L10-18.

Clayton R. N. and Mayeda T. K. (1984) *Earth and Planetary Science, 67,* L151-161.

Cohen B. and Coker R (2000) *Icarus, 145,* 369-381.

Cruikshank D., Dalle Ore C., Roush T. L., Geballe T., Owen T. et al. (2001) *Icarus, 153,* 348-360.

Czechowski L. and Leliwa-Kopystyski J. (2002) *Adv. Space Res., 29,* 751-756.

Davies J. K., Roush T. L., Cruikshank D. P., Bartholomew M. J., Geballe T. R., Owen T., and de Bergh C. (1997) *Icarus, 127,* 238-245.

Dumas C., Owen T., and Barucci M. A. (1998) *Icarus, 133,* 221-232.

Emery J. and Brown R. (2004) *Icarus, 170,* 131-152.

Fanale F. P. and Salvail J. R. 1989, *Icarus, 82,* 97-110.

Fernández J. A., Gallardo, T., and Brunini, A. (2002) *Icarus, 159,* 358-368.

Fernández Y., Sheppard S., and Jewitt D. (2003) *Astron. J., 126,* 1563-1574.

Fruh-Green G., Kelley D., Bernasconi S., Karson J., Ludwig K. et al. (2003) *Science, 301,* 495-498.

Ghosh A., Weidenshilling S. and McSween H. (2003) *Meteorit. Planet. Sci., 38,* 711-724.

Grimm R. E. and McSween H. Y. (1989) *Icarus, 82,* 244-280.

Grimm R. E. and McSween, H. Y. 1993, *Science, 259,* 653-655.

Grossman J. and Rubin A. (1999) *Lunar and Planetary Science*

Conference XXX, abstract 1639.
Grossman J. and Brearley A. J. (2003) *Lunar and Planetary Science Conference XXXIV*, abstract 1584.
Grossman J., Alexander C. M. OD. Wang J. and Brearley A. J. (2000) *Meteorit. Planet. Sci., 35*, 467-486.
Haruyama J., Yamamoto T., Mizutani H., and Greenberg J. M. (1993) *J. Geophys. Res., 98, E8*, 15,079
Hanowski N. and Brearley A. J. (2001) *Meteorit. Planet. Sci., 35*, 1291-1308.
Herndon J. M. and Herndon M. A. (1977) *Meteoritics, 12*, 459-465.
Hiroi T., Zolensky M. E. and Pieters C. M. (2001) *Science, 293*, 2234-2236.
Hiroi T. and Hasegawa S. (2003) *Antarctic Meteorite Research, 16*, 176-184.
Hsieh H., Jewitt D. and Fernández Y. (2004) *Astron. J., 127*, 2997-3017.
Hsieh H. and Jewitt D. (2006) *Science*, in press.
Hutcheon I., Krot A., Keil K., Phinney D., and Scott E. (1998) *Science, 282*, 1865-1867.
Jakosky B. M. and Shock E. L. (1998) *J. Geophys. Res., 103*, 19359-19364.
Jewitt D. (2002) *Astron. J., 123* 1039-1049.
Jewitt D. (2005) In *Comets II*, (M. Festou, H. Weaver and H. Keller eds.), pp 659-676. Univ. of Arizona, Tucson.
Jewitt D. and Luu J. (1990) *Astron. J., 100*, 933-944.
Jewitt D. and Luu J. (2004) *Nature, 432*, 731-733.
Jewitt D., Sheppard S., and Porco C. (2004) *Jupiter. The Planet, Satellites and Magnetosphere*, (F. Bagenal, W. McKinnon eds), pp. 263-280. Univ. of Arizona, Tucson.
Jones T., Lebofsky L., Lewis J., and Marley M. (1990) *Icarus, 88*, 172-192.
Kawakita H., Watanabe J.-I., Ootsubo T., Nakamura R., Fuse T., Takato N., Sasaki S., and Sasaki T. (2004) *Astrophys. J., 601*, L191-194.
Keil K. (2000) *Planet. Space Sci., 48*, 887-903.
Kelley D., Karson J., Blackman D., Fruh-Green G., Butterfield D. et al. (2001) *Nature, 412*, 145-149.
Kemper F., Jäger C., Waters L, Henning T., Molster F., Barlow M., Lim T., and de Koter, A. (2002) *Nature, 415*, 295-297.
Kenyon S. J. (2002) *PASP, 114*, 265-283.
Kerridge J. F., Mackay A. L., and Boynton, W. V. (1979) *Science, 205*, 395-397.
King T., Clark R., Calvin W., Sherman D., and Brown R. (1992) *Science, 255*, 1551-1553.
Krot A., Brearley A., Ulyanov A., Biryukov V., Swindle T., Keil K., Mittlefehldt D., Scott E., Clayton R., and Mayeda T. (1999) *Meteorit. Planet. Sci., 34*, 6790.
Krot A. N., Hutcheon I., Yurimoto H., Cuzzi J., McKeegan K. et al. (2005) *Astrophys. J., 622*, 1333-1342.
Lebofsky L., Feierberg M., Tokunaga A., Larson H., and Johnson J. (1981) *Icarus, 48*, 453-459.
Lee T., Papanastassiou D. A., and Wasserburg G. J. (1976) *Geophys. Res. Lett., 3*, 41-44.
Levison H., Terrell D., Wiegert P., Dones L., and Duncan M. (2006) *Icarus*, in press.
Lisse C., VanCleve J., Adams A., A'Hearn M., Belton M. et al. (2006) *Science*, submitted (January 9).
Luu J., Jewitt D., and Cloutis, E. (1994) *Icarus, 109*, 133-144.
Lyons J. R. and Young E. D. (2005) *Nature, 435*, 317-320.
MacPherson G. J., Davis A. M., and Zinner E. K. (1995) *Meteoritics, 30*, 365.
Marchis, F. et al. (2006) *Nature, 439*, 565-567.
Marzari F., Davis, D., and Vanzani V. (1995) *Icarus, 113*, 168-187.
Mastrapa R., Moore M., Hudson R., Ferrante R., and Brown R. (2005) AAS/Division for Planetary Sciences Meeting Abstracts, 37.
McCord T. B. and Sotin C. (2005) *J. Geophys. Res. (Planets), 110*, E05009
McSween H. Y. (1979) *Geochim. Cosmochim. Acta, 43*, 1761-1770.
McSween H., Ghosh A., Grimm R., Wilson L., and Young E. (2002) In *Asteroids III* (W. Bottke et al., eds), pp. 559-571, Univ. of Arizona, Tucson.
Meier R. and Owen T. C. (1999) *Space Sci. Rev., 90*, 33-44.
Meier R. et al. (1998a) *Science, 279*, 842-844.
Meier R. et al. (1998b) *Science, 279*, 1707-1709.
Merk R. and Prialnik D. (2003) *Earth, Moon, and Planets, 92*, 359-374.
Mostefaoui S., Lugmair G. W., Hoppe P., and El Goresy A. (2004) *New Astronomy Review, 48*, 155-159.
Morbidelli A. et al. (2000) *Meteorit. Planet. Sci., 35*, 1309-1320.
Morbidelli A., Levison H., Tsiganis K., and Gomes R. (2005) *Nature, 435*, 462-465.
Nakamura T., Noguchi T., Zolensky M. and Tanaka M. (2003) *Earth and Planetary Science, 207*, L83-101.
Notesco G. and Bar-Nun A. (2005) *Icarus 175*, 546-550.
Owen T. and Bar-Nun A. (1995) *Icarus 116*, 215-226.
Pollack J., Hollenbach D., Beckwith S., Simonelli D., Roush T., and Fong W. (1994) *Astrophys. J. 421*, 615-639.
Prialnik D. (1992) *Astrophys. J., 388*, 196-202.
Prialnik D. and Podolak M. (1995) *Icarus, 117*, 420-430.
Prialnik D., Benkhoff J., and Podolak M. (2005) In *Comets II*, (M. Festou, H. Weaver and H. Keller, eds.), pp. 359-387. Univ. Arizona, Tucson.
Prinn R. G. and Fegley, B. (1981) *Astrophys. J., 249*, 308-317.
Prinn R. G. and Fegley, B. (1987) *Ann. Rev. of Earth and Planetary Sciences, 15*, 171-212.
Rietmeijer F. (1991) *Earth and Planetary Science, 102*, L148-157.
Rietmeijer F. (1998) In *Mineralogy: Planetary Materials 36*, (J. J. Papike, ed.). pp. 201-287. Mineralogical Society of America, Washington, D. C., USA.
Rivkin A., Howell E., Vilas F., and Lebofsky L. (2002) In *Asteroids III*, (W. Bottke et al. eds), pp.235-253. Univ. Arizona, Tucson.
Sasselov D. D. and Lecar, M. (2000) *Astrophys. J., 528*, 995-998.
Starukhina L. (2001) *J. Geophys. Res., 106*, 14701-14710.
Stevenson D. J. and Lunine J. I. (1988) *Icarus, 75*, 146-155.
Sykes M. V. and Walker R. G. (1992) *Icarus, 95*, 180-210.
Sykes M. V., Lebofsky L. A., Hunten D. M., and Low F. (1986) *Science, 232*, 1115-1117.
Thomas P., Parker J., McFadden L., Russell C., Stern S., Sykes M., and Young E. (2005) *Nature, 437*, 224-227.
Tonui E. K., Zolenksy M. E., Lipschutz M. E., Wang M-S and Nakamura T. (2003) *Meteorit. Planet. Sci., 38*, 269-292.
Toppani A., Robert F., Libeourel G., de Donato P., Barres O., d'Hendecourt L., and Ghanbaja J. (2005) *Nature, 437*, 1121-1124.
Toth I. (2000) *Astron. Astrophys., 360*, 375-380.
Vernazza P. et al. (2005) *Astron. Astrophys., 436*, 1113 -1121.
Vilas F. (1994) *Icarus, 111*, 456-467.
Wallis M. K. (1980) *Nature 284*, 431-433.
Whipple F. L. 1950, *Astrophys. J., 111*, 375-394.
Wilson L., Keil K., Browning L., Krot A. and Bourcier W. (1999)

Meteorit. Planet. Sci., 34, 541-557.
Yabushita S. (1993) *Mon. Not. R. Astron. Soc., 260*, 819-825.
Young E. D., Zhang K. K., and Schubert G. (2003) *Earth and Planetary Science, 213*, L249-259.
Zolensky M., Bourcier W. and Gooding J. (1989) *Icarus, 78*, 411-425.
Zolensky M. E., Barrett R. A. and Browning L. B. (1993) *Geochimica et Cosmochimica Acta, 57*, 3123-3148.
Zolensky M. E., Gibson K. E. Jr. Lofgren E. G. Morris V. R. and Yang V. S. (1998) *23rd Symposium on Antarctic Meteorites, NIPR* 189-191.
Zolensky M. E., Bodnar R. J. and Rubin A. E. (1999) *Meteorit. Planet. Sci., 34 (Suppl.)* A124.